

Fission Barriers at High Angular Momentum and the Ground State Rotational Band of the Nucleus ^{254}No

J. L. Egido and L. M. Robledo

Departamento de Física Teórica, Universidad Autónoma de Madrid, 28049 Madrid, Spain

(Received 27 March 2000)

We study the superheavy nucleus ^{254}No in the framework of the Hartree-Fock-Bogoliubov approximation with the finite-range density-dependent Gogny force, at zero and high angular momentum. The properties of the ground state rotational band and the fission barriers are discussed as a function of angular momentum. We found a two-humped barrier up to spin values of $(30-40)\hbar$ and a one-humped barrier for higher spins. We reproduce fairly well with the binding energy, the ground state deformation, the γ -ray energies, and the bound on the fission barrier height measured at high spin.

PACS numbers: 27.90.+b, 21.10.Hw, 21.60.Jz, 24.75.+i

Very recently [1–3], the combination of highly efficient Ge detector arrays with a recoil fragment separator has allowed the identification of γ rays from the ground state rotational band of ^{254}No . In particular, in Ref. [3], the nucleus ^{254}No was populated up to spin $22\hbar$ and excitation energy ~ 8 MeV employing the cold fusion reaction $^{208}\text{Pb}(^{48}\text{Ca}, 2n)$. From their analysis the authors conclude that at high spin the fission barrier height is ≥ 5 MeV and that the shell-correction energy still persists. This type of experiment is very important for the understanding of the nuclear interaction: the nucleus ^{254}No belongs to the class of superheavy or transfermium nuclei ($Z > 100$), the stability of which is not due to the macroscopic properties of the nuclear interaction but rather to the more subtle shell effects underlying the nuclear force. As a consequence, the properties of its ground and excited states are an excellent testing ground for the effective interactions used nowadays in the description of nuclear structure properties. In addition, this type of experiment, poses a big challenge to any parameter-free theoretical description, because bulk properties, such as ground state deformations, fission barriers and binding energy, have to be reproduced together with sensitive spectroscopic γ -ray energies (among others).

The purpose of this Letter is to present a thorough theoretical investigation of the nucleus ^{254}No , including an analysis of the fission barriers at zero and high spin to investigate the stability of this nucleus. In our study we shall use the finite-range density-dependent Gogny force [4,5] (D1S parametrization [6]) which provides a good description of nuclear bulk properties [5,7] and fission barriers [8] at zero angular momentum. Although no high spin data were taken into account in the fit of the Gogny force, it provides a good description of properties of the normal deformed [9] and superdeformed ground rotational bands [10] at high spins. We expect, therefore, that our fission barrier calculations will provide reliable predictions. In addition to the fission barriers, we will also present results for the measured ground state band as well as the predictions for a hypothetical low-lying superdeformed band. The calculations have been done in the Hartree-

Fock-Bogoliubov (HFB) approximation. The angular momentum and particle number quantum numbers have been taken into account on average, i.e., the expression $\langle \phi | \hat{H}' | \phi \rangle = \langle \phi | \hat{H} | \phi \rangle - \lambda \langle \phi | \hat{N} | \phi \rangle - \omega \langle \phi | \hat{J}_x | \phi \rangle$ has been minimized. The wave function $|\phi\rangle$ is of the HFB type and λ and ω are the Lagrange multipliers determined by the constraints $\langle \phi | \hat{N} | \phi \rangle = N$ and $\langle \phi | \hat{J}_x | \phi \rangle = \sqrt{I(I+1)}$ on the particle number and the angular momentum, respectively [9]. To study the fission barriers an additional constraint on the quadrupole moment was considered. Further correlations, such as the zero point energy (ZPE) arising from symmetries broken in the HFB approach, have also been considered.

In the calculations a harmonic oscillator (HO) basis has been used. The basis has been truncated using the condition $a_x n_x + a_y n_y + a_z n_z < N_0$, where n_x , n_y , and n_z are the HO quantum numbers. The parameters $a_x = a_y = q^{1/3}$ and $a_z = q^{-2/3}$ are related to the nuclear axis ratio by $q = R_z/R_x$. In our calculations we have chosen the values $q = 1.5$ (which is large enough to describe the fission barrier region) and $N_0 = 15.1$ or 17.1 , depending on the calculation. As a check of our calculations and to analyze the role played by different symmetries, we have performed several calculations at zero angular momentum. In particular, in these checks we use an axially symmetric code and a triaxial one. In Fig. 1 we present the energy as a function of the mass quadrupole moment with $N_0 = 17.1$ for the axially symmetric case (curve denoted HFB). Along the fission path we observe two minima, normal deformed (ND) at $Q_{20} = 16$ b and, about 2 MeV above, superdeformed (SD) at $Q_{20} = 53$ b, as well as two humps, one at $Q_{20} = 32.5$ b and the other at $Q_{20} = 72$ b. Up to $Q_{20} = 70$ b, the HFB solutions are reflection symmetric (RS) but from that point on they develop an octupole moment, Q_{30} , different from zero, i.e., they become reflection asymmetric (RA). For comparison the RS solution is also shown in Fig. 1 [line denoted HFB ($Q_{30} = 0$)]. As we can see, the octupole shapes are not relevant at the ND and SD minima but play an important role in narrowing the width of the fission barrier. It is interesting to note that

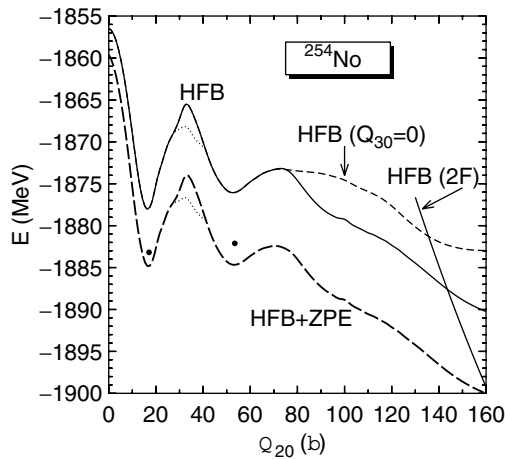


FIG. 1. Fission barriers at zero angular momentum in different approaches: axially symmetric HFB (solid line), axially symmetric HFB with reflection symmetry (thin dashed line), triaxial HFB with reflection symmetry (dotted lines), axially symmetric HFB plus ZPE (thick dashed line). The solid circles in the minima represent the axially symmetric HFB energy plus the ZPE's evaluated with exact projection.

the inclusion of RA shapes affects the width of the barrier but not the height. To evaluate the effects of the triaxiality, additional calculations with a triaxial code (no RA shapes allowed) have been performed. The results are displayed as the dotted lines. We observe that the triaxiality effects are noticeable only in the region of the first saddle point. This conclusion cannot be generalized, obviously, to spins different from zero. The calculations just discussed correspond to one-fragment configurations. In addition to these solutions we also obtain two-fragment solutions [curve denoted HFB (2F)]. For a given value of the quadrupole moment it is possible to reach the two-fragment solution, starting from the one-fragment solution, by increasing the hexadecupole moment. The two-fragment configuration shown corresponds to the fragments ^{124}Sn and ^{130}Te . To check the convergence of the calculations with the number of oscillator shells we have calculated the fission barriers with $N_0 = 15.1, 16.1,$ and 17.1 oscillator shells. The positions of the minima and the humps are not affected by the basis size (only at very large values of the quadrupole moment can one find small differences between the considered N_0 values). In particular we obtain, for the three N_0 values studied, the barrier heights of 12.46, 12.49, and 12.40 MeV for the first barrier (triaxial effects which make them smaller by a few MeV are not included) and 3.42, 3.09, and 3.03 MeV for the second barrier. The widths of the barriers do not change much either with the number of shells.

It is well known that ZPE corrections are important along the fission path. The most important of these corrections have their origin in the fact that the HFB wave functions are not eigenstates of the angular momentum and the particle number operators. In the frame of a projection after variation theory, to evaluate the corrections, one

should calculate the projected energy after the HFB minimization. Since the exact projection is very complicated, one usually has to resort to approximate methods; the most common one can be derived for large deformations. In this case it can be shown (see, for example, Ref. [11]) that the ZPE can be written as $\langle \Delta \hat{J}^2 \rangle / (2J_Y)$ for the rotational energy correction and $\langle \Delta \hat{N}^2 \rangle / (2J_Y^N)$ for the particle number case. The quantities $\langle \Delta \hat{J}^2 \rangle$ and $\langle \Delta \hat{N}^2 \rangle$ are the fluctuations associated with the angular momentum and the particle number operators in the HFB wave function. The Yoccoz moments of inertia J_Y and J_Y^N have been computed in the “cranking” approximation [11]. The consideration of these corrections provides the curve labeled HFB + ZPE in Fig. 1. The main effect of this correction is a shift of the curve as a whole. A more careful look reveals, however, that the energy of the SD minimum has been lowered somewhat more than the ND minimum. With ZPE corrections the height of the first barrier, in the axial approximation, is about 11 MeV, in good agreement with the axial calculations of [12,13]. Concerning the possibility to experimentally observe the SD minimum, one has to consider that since the barrier seen by the SD minimum is not very high it is not clear whether the fission half-time will be long enough to allow decays along the SD band. To calculate the excitation energy of the SD minimum in a better approximation we have performed exact angular momentum [14] and particle number [15] projections in both minima. We obtain a correction of 2.952 MeV (ND minimum) and 3.947 MeV (SD minimum) from the angular momentum projection. These numbers are approximately $0.7 \times \langle \Delta \hat{J}^2 \rangle / (2J_Y)$, the factor 0.7 being in good agreement with the results of [16]. From the particle number projection we obtain 2.203 MeV (ND minimum) and 2.084 MeV (SD minimum). These numbers show that the main correction to the HFB results stems from the rotational part since the particle number correction is very similar in both minima. After this correction, the SD minimum lies 0.87 MeV above the ND one. The energy of both minima is shown in Fig. 1 by filled circles. The height of the first barrier with triaxiality effects and exact ZPE's is 8.66 MeV. The binding energy obtained in the HFB calculation is 1878.028 MeV and, with exact projected ZPE's 1883.183 MeV. This value is in good agreement with the experimental result 1885.598 MeV [17].

We now discuss the properties of the fission barriers at high angular momentum. In Fig. 2 we present the fission barriers at the indicated spin values. The calculations have been performed in the cranked HFB approximation with $N_0 = 15.1$ shells without consideration of ZPE corrections. Since the computer code is restricted to RS shapes, we limited our calculations up to the saddle point on the second barrier, i.e., the region where we know that octupolar shapes do not play a significant role. Concerning the energies of both minima, we find that the SD minimum falls below the ND one for $I = 24\hbar$ ($I = 16\hbar$ if ZPE corrections are included). An overall effect that we observe

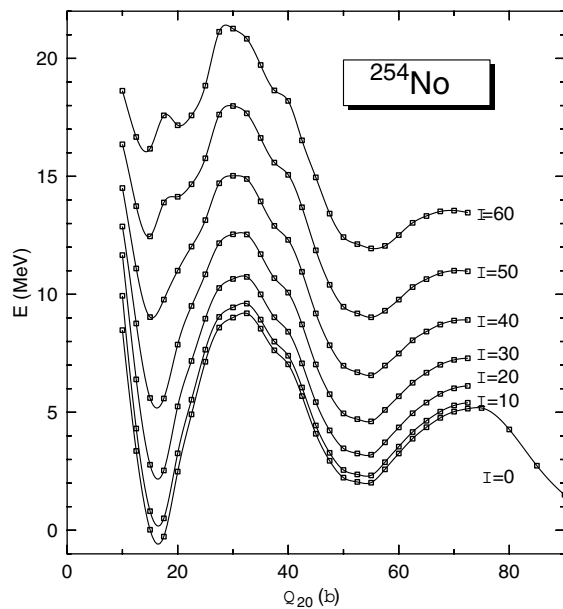


FIG. 2. Fission barriers for different spin values. The energy origin has been fixed by subtraction of a given value to all energies. The angular momentum I is given in units of \hbar .

in the barriers is that the height of both barriers diminishes with increasing spin values. Experimentally, it was found that for spin $I \approx 20\hbar$ the barrier height is ≥ 5 MeV which is confirmed by our calculations. We find that up to $I = 30\hbar$ no big changes are observed in the shape of the barriers. The first qualitative change takes place between spin $I = 30\hbar$ and $I = 40\hbar$. As we can see for $I \geq 40\hbar$ the ND minimum lies above the second saddle point, i.e., the barrier becomes one humped instead of two humped, indicating a decrease in the barrier width and height. An-

other important issue is the broadening of the well around the ND minimum at very high spins. This can be clearly seen for $I \geq 40\hbar$. The direct consequence is that the fission barrier gets thinner for those spin values. The last two effects combined indicate a clear increase of the barrier penetrability for spins $I \geq 40\hbar$. The inclusion of the ZPE discussed above may play a role in diminishing this spin value although we do not expect that the qualitative aspects will change.

We shall now discuss the most relevant properties of the ND and the hypothetical SD band, built on the corresponding minima. In Fig. 3(a) the γ -ray energies, $E_\gamma(I) = E(I) - E(I - 2)$, along the ND and SD bands are depicted. In the theoretical ND band, in addition to the very good agreement with the experiment, we observe a small irregularity at $I \sim 30\hbar$ and a bigger one at $I \sim 38\hbar$. As can be seen in the plot of $J^{(1)}$ in the same figure they correspond to an upbending and a backbending, respectively. The γ -ray energies within the SD band are smaller and behave like the ones of a rigid rotor with a moment of inertia of $J^{(1)} = 173.3\hbar^2 \text{ MeV}^{-1}$, which is very close to the moment of inertia ($J^{(1)} = 170\hbar^2 \text{ MeV}^{-1}$) of a rigid body with the deformation of this nucleus (see below). The large electron conversion of these γ rays in the measured angular momentum region may explain why they have not been observed in the experiments [1,3]. The pairing energy, $E_{pp} = \frac{1}{2} \text{Tr}(\Delta\kappa)$, for protons and neutrons is depicted in 3(b). Along the ground state band we find larger pairing correlations for protons than for neutrons, and we observe the usual Coriolis antipairing effect up to the backbending point. From this point on, the neutron pairing energy increases again, indicating that the crossing band still has some pairing correlations left. The SD band has larger

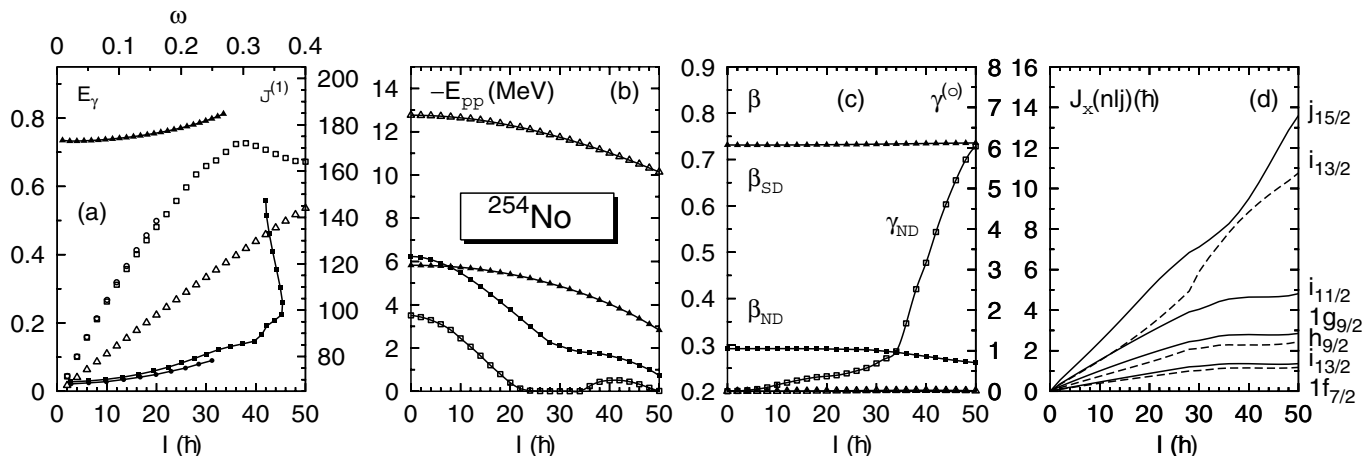


FIG. 3. Properties of the ND and SD bands in ^{254}No . (a) E_γ values in MeV (left axis) versus the spin (bottom axis), and $J^{(1)}$ values in $\hbar^2 \text{ MeV}^{-1}$ (right axis) versus ω in MeV (top axis). ND band: empty (filled) circles, experimental E_γ ($J^{(1)}$) values [1–3], empty (filled) squares, E_γ ($J^{(1)}$) theoretical results. SD band: empty (filled) triangles, E_γ ($J^{(1)}$) theoretical values. (b) Pairing energies. ND band: filled (open) squares for protons (neutrons). SD band: filled (open) triangles for protons (neutrons). (c) β and γ deformation parameters. Ground state band: filled (open) squares for β (γ). (d) Contribution of the spherical orbitals to the total angular momentum along the ND band; solid (dashed) lines for neutrons (protons).

pairing correlations than the ND band and, opposite to the ND case, the neutron system is stronger correlated than the proton system. The SD band has a moment of inertia about 2.5 times larger than the one in the ND band. Therefore, the angular frequency needed to generate a given value of the angular momentum is a factor of 2.5 smaller than the one in the ND minimum. As a consequence, at a given spin I , the Coriolis force is much smaller in the SD band than in the ND band. This fact explains why at high spins the pairing correlations are less quenched in the SD minimum than in the ND minimum. The β and γ deformation parameters are depicted in 3(c). In the ND band, β is practically constant as a function of I up to the backbending and starts decreasing from there on. This antistretching effect is caused by the Coriolis force. Our theoretical value for the deformation is $\beta = 0.29$, in good agreement with the experimental value $\beta = 0.27(2)$ [1]. Concerning γ , it never exceeds 0.5° before the backbending, but it steadily increases for higher I values up to 6.0° at $I = 50\hbar$. This behavior indicates that particle alignment has taken place [9]. For the SD band we find at low spins $\beta = 0.731$ and $\gamma \approx 0^\circ$. At high spin, γ always remains very small and β decreases very slowly. Again, due to the smaller angular frequencies, the Coriolis antistretching effect is smaller in this band as compared to the ND band.

In order to disentangle the origins of the upbending at $I \sim 30\hbar$ and the backbending at $I \sim 38\hbar$, we computed the quantity $J_x(a, I) = (2j + 1)^{-1} \sum_{m, m'} (J_x)_{am, am'} \times \langle \phi(I) | c_{am}^+ c_{am'} | \phi(I) \rangle$, with $a = (nlj)$, which measures the contribution of the spherical orbit with quantum numbers a to the total angular momentum. These quantities are plotted as a function of I for the most relevant values of lj in 3(d). We see that the $\pi i_{13/2}$ orbital starts aligning at $I \sim 28\hbar$ causing the upbending at $I \sim 30\hbar$, whereas the orbital responsible for the backbending is the $\nu j_{15/2}$ which starts aligning at $I \sim 36\hbar$. Finally, to make sure that the agreement with experiment obtained in this nucleus is not accidental, we have also computed the four lowest γ -ray energies measured in the rotational ground state band of ^{256}Fm . We obtain 48.9, 113.1, 175.6, and 235.3 keV to be compared with the experimental values 48.3, 111.6, 172.6, and 231.1 keV [18,19]. For ^{254}Fm , we obtain 46.6 and 108.1 keV to be compared with the experimental values 45 and 104 keV [19]. Again we find good agreement with the scarce experimental results.

In conclusion, we have presented a microscopic description of the nucleus ^{254}No with the Gogny force, one of the most successful effective interactions used nowadays

in nuclear structure calculations. We have calculated for the first time the fission barriers at high spin with effective forces and found that the experimental barrier height limit [1] is within our predictions. We have found a two-humped barrier for spin values from $I = 0\hbar$ up to $I = (30-40)\hbar$ and a one-humped barrier for larger spins. From the shape of the barriers we conclude that the stability of this nucleus may persist up to spin values of $\approx 40\hbar$ or even higher. We have reproduced very nicely the measured γ -ray energies along the ground state rotational band. We have predicted, furthermore, an upbending and a backbending in this band. The ground state deformation and the binding energy of this nucleus are also in good agreement with the experimental values.

This work has been supported in part by the DGEIC, Spain, under Project No. PB97-0023. We thank M. Anguiano and R. R. Rodriguez Guzman for their assistance in the calculation of the projected energies.

-
- [1] P. Reiter *et al.*, Phys. Rev. Lett. **82**, 509 (1999).
 - [2] M. Leino *et al.*, Eur. Phys. J. A **6**, 63 (1999).
 - [3] P. Reiter *et al.*, Phys. Rev. Lett. **84**, 3542 (2000).
 - [4] D. Gogny, in *Nuclear Selfconsistent Fields*, edited by G. Ripka and M. Porneuf (North-Holland, Amsterdam, 1975).
 - [5] J. Dechargé and D. Gogny, Phys. Rev. C **21**, 1568 (1980).
 - [6] J. F. Berger, M. Girod, and D. Gogny, Comput. Phys. Commun. **63**, 365 (1991).
 - [7] M. Girod and B. Grammaticos, Phys. Rev. C **27**, 2317 (1983).
 - [8] J. F. Berger, M. Girod, and D. Gogny, Nucl. Phys. **A428**, 23c (1984).
 - [9] J. L. Egido and L. M. Robledo, Phys. Rev. Lett. **70**, 2876 (1993).
 - [10] A. Valor, J. L. Egido, and L. M. Robledo, Nucl. Phys. **A665**, 46 (2000).
 - [11] P. Ring and P. Shuck, *The Nuclear Many Body Problem* (Springer-Verlag, Berlin, 1980).
 - [12] S. Cwiok *et al.*, Nucl. Phys. **A410**, 254 (1983).
 - [13] A. Staszczak *et al.*, Nucl. Phys. **A504**, 589 (1989).
 - [14] R. R. Rodriguez-Guzmán, J. L. Egido, and L. M. Robledo, Phys. Lett. B **474**, 15 (2000).
 - [15] M. Anguiano, J. L. Egido, and L. M. Robledo (to be published).
 - [16] M. Girod *et al.*, Phys. Rev. C **45**, R1420 (1992).
 - [17] G. Audi and A. H. Wapstra, Nucl. Phys. **A595**, 409 (1995).
 - [18] H. L. Hall *et al.*, Phys. Rev. C **39**, 1866 (1989).
 - [19] K. J. Moody *et al.*, Nucl. Phys. **A563**, 21 (1993).